SCIENCE CHINA
Information Sciences

• RESEARCH PAPER •

July 2018, Vol. 61 070222:1–070222:12
https://doi.org/10.1007/s11432-017-9368-x

Special Focus on Advances in Disturbance/Uncertainty Estimation and Attenuation Techniques With Applications

Robust disturbance rejection for a fractional-order system based on equivalent-input-disturbance approach

Ruijuan LIU[1*], Jinhua SHE[2,3,4], Min WU[2,4], Fenfang ZHU[5] & Zhuoyun NIE[5]

[1]*School of Applied Mathematics, Xiamen University of Technology, Xiamen* 361024*, China;*
[2]*School of Automation, China University of Geosciences, Wuhan* 430074*, China;*
[3]*School of Engineering, Tokyo University of Technology, Tokyo* 192-0982*, Japan;*
[4]*Hubei Key Laboratory of Advanced Control and Intelligent Automation for Complex Systems, Wuhan* 430074*, China;*
[5]*School of Information Science and Engineering, National Huaqiao University, Xiamen* 361021*, China*

Received 29 September 2017/Revised 18 December 2017/Accepted 25 January 2018/Published online 24 May 2018

Abstract This paper presents a disturbance rejection method that is based on the equivalent-input-disturbance approach for uncertain fractional-order (FO) systems. An FO observer is used to reconstruct the plant states and estimate the disturbances. A disturbance estimator is incorporated in the construction of the FO control system to actively compensate for the entire disturbance. A robust stability condition for the control system and the parameters of the controller are derived using an indirect Lyapunov method. The presented method effectively rejects disturbances and handles modeling uncertainties without requiring prior knowledge of the disturbance. Comparison simulations on both numerical and practical examples demonstrate the effectiveness of the proposed method.

Keywords fractional-order system, disturbance rejection, equivalent-input-disturbance, uncertain system, Lyapunov method, state observer, stability

Citation Liu R J, She J H, Wu M, et al. Robust disturbance rejection for a fractional-order system based on equivalent-input-disturbance approach. Sci China Inf Sci, 2018, 61(7): 070222, https://doi.org/10.1007/s11432-017-9368-x

1 Introduction

During the past two decades, fractional-order (FO) calculus has attracted increasing interest in many fields, such as physics, chemistry, and engineering. Compared with integer-order (IO) calculus, FO calculus has several advantages in the study of control systems. First, FO derivatives have finite- and infinite-dimensional characteristics, which help solve the description problem of distributed parameter systems [1]. Thus, FO models describe the dynamic process and properties of the real system more accurately. Second, FO controllers, such as CRONE, TID, and FO PID controllers, which have been applied in practical engineering applications, constantly exhibit good control performance in the FO system (FOS) because they have considerable degrees of freedom [2–4].

In 1996, Matignon [5] presented the bounded-input-bounded-output stability condition for the FOS, which offers a theoretical basis for the stability analysis and controller design of the FOS. Subsequently, researchers have proposed numerous linear-matrix-inequality (LMI) stability and stabilization conditions

* Corresponding author (email: liuruijuan0313@163.com)

to ensure the robust stability of several classes of FOSs [6, 7]. A Lyapunov method was introduced in [8] for analyzing the stability of nonlinear systems. However, this method constructs a Lyapunov functional using pseudo-state, thus limiting the control design of the FOS. To overcome this problem, Trigeassou [9] presented an indirect Lyapunov method for the stability of fractional differential equations. The real states in the equivalent model are used to construct the energy function [10]. And this method does not need to calculate the fractional derivative of the Lyapunov function.

Researchers have developed several advanced techniques for the control design of the FOS on the basis of its stability theories. These techniques include the sliding mode control (SMC) for uncertain and nonlinear FOSs [11, 12], active disturbance rejection control (ADRC) for nonlinear FOSs and FO chaotic systems [13, 14], and adaptive control for FOSs [15].

As an important objective in the design of a control system, disturbance rejection problem also attracts attention. Several disturbance rejection problems have recently been reported in the literature. ADRC was first used for the FOS in [16]. The closed-loop system is considered a second-order system, and FO is regarded as a part of the total disturbance, which is compensated by an external state observer (ESO). Li et al. [17] developed a fractional ADRC method using the fractional ESO, which estimates the total disturbance and dynamic states of the FO. Periodic disturbance for the FOS is considered on the basis of an adaptive orthogonal signal generator [18]. An SMC scheme based on a disturbance observer is introduced for a class of nonlinear FOSs with mismatched disturbances, where the derivative of the external disturbance is assumed to converge to zero [19].

However, many problems are still found in the disturbance rejection of the FOS. The disturbance rejection effect is constantly unsatisfactory. Moreover, several methods are suitable for only part of the FOS or certain types of disturbances. The disturbance rejection problem becomes increasingly difficult when modeling uncertainty is considered. The equivalent-input-disturbance (EID) approach overcomes these difficulties in IO systems [20]. This approach is effective in working with external disturbances and modeling uncertainties without prior information of the disturbances [21].

Motivated by prior work, the current study presents a robust disturbance rejection method for uncertain FOSs that is based on the EID approach. The configuration of the FO control system contains an FO state observer and a disturbance estimator. A robust stability condition of the control system and the design of the parameters are derived by applying an indirect Lyapunov method. The proposed method is effective in handling uncertainties and rejecting any type of unknown disturbance for an FOS. Moreover, the measurement noise is also well processed due to the FO filter. Comparison simulations on both numerical and practical examples demonstrate the validity of the method.

Throughout this paper, $\mathbb{R}^n$ and $\mathbb{R}^{m\times n}$ stand for an n-dimensional Euclidean space and the set of all $m \times n$ real matrices, respectively. We denote by X^{T} the transpose of X. I and 0 stand for the identity matrix and the null matrix of appropriate dimensions. The notation $A > 0$ ($A < 0$) with A being a symmetric matrix means that the matrix A is positive (negative) definite. And $\left[\begin{smallmatrix} X & Y \\ * & Z \end{smallmatrix}\right]$ stands for $\left[\begin{smallmatrix} X & Y \\ Y^{\mathrm{T}} & Z \end{smallmatrix}\right]$.

2 Preliminaries and problem formulation

In this section, some definitions and lemmas are introduced for the control design of the FOS.

Definition 1 ([3])**.** The Caputo fractional derivative of the function $f(t)$ with starting point $t_0 = 0$ is defined by

$$ {}_0D_t^{\alpha} f(t) = \frac{1}{\Gamma(m-\alpha)} \int_0^t \frac{f^{(m)}(\tau)}{(t-\tau)^{\alpha+1-m}} \mathrm{d}\tau, \tag{1} $$

where $\Gamma(\cdot)$ is the Gamma function, $\Gamma(z) = \int_0^{\infty} \mathrm{e}^{-z} t^{z-1} \mathrm{d}t$, and m is an integer satisfying $m - 1 < \alpha \leqslant m$.

Definition 2 ([9])**.** Let $h(t)$ be the impulse response of a linear system. The diffusive representation (or frequency weighting function) of $h(t)$ is called $\mu(\omega)$ with the following relation

$$ h(t) = \int_0^{\infty} \mu(\omega) \mathrm{e}^{-\omega t} \mathrm{d}\omega, \tag{2} $$

where $\mu(\omega) = \frac{\sin(\alpha\pi)}{\pi}\omega^{-\alpha}$.

Lemma 1 ([9]). The fractional-order differential equation

$$ {}_0D_t^{\alpha}x(t) = Ax(t) $$

due to the continuous frequency distributed model of the fractional integrator, can be expressed as

$$ \begin{cases} \dfrac{\partial z(\omega,t)}{\partial t} = -\omega z(\omega,t) + Ax(t), \\ x(t) = \int_0^{\infty} \mu(\omega) z(\omega,t)\mathrm{d}\omega, \end{cases} \tag{3} $$

where $z(\omega,t)$ is the continuous distributed state variable, and $\mu(\omega)$ is the frequency weighting function of the state variable $z(\omega,t)$, which is defined in Definition 2.

Lemma 2 ([22]). Given matrices Y, D and E of appropriate dimensions, $Y + DFE + E^{\mathrm{T}}F^{\mathrm{T}}D^{\mathrm{T}} < 0$ holds for all F satisfying $FF^{\mathrm{T}} < I$, if and only if there exists an $\varepsilon > 0$ such that $Y + \varepsilon DD^{\mathrm{T}} + \varepsilon^{-1}E^{\mathrm{T}}E < 0$.

Lemma 3 ([23]). For a given matrix $\Pi \in \mathbb{R}^{p\times n}$ with $\mathrm{rank}(\Pi) = p$, there exists a matrix $\bar{X} \in \mathbb{R}^{p\times p}$ such that $\Pi X = \bar{X}\Pi$ holds for any $X \in \mathbb{R}^{n\times n}$, if and only if X can be decomposed as

$$ X = W\mathrm{diag}\{\bar{X}_{11}, \bar{X}_{22}\}W^{\mathrm{T}}, \tag{4} $$

where $W \in \mathbb{R}^{n\times n}$ is an orthogonal matrix, $\bar{X}_{11} \in \mathbb{R}^{p\times p}$, and $\bar{X}_{22} \in \mathbb{R}^{(n-p)\times(n-p)}$.

Lemma 4 (Schur complement [24]). For a given symmetric matrix

$$ \Sigma = \begin{bmatrix} \Sigma_{11} & \Sigma_{12} \\ * & \Sigma_{22} \end{bmatrix}, \tag{5} $$

the following statements are equivalent:

(1) $\Sigma < 0$;

(2) $\Sigma_{11} < 0$ and $\Sigma_{22} - \Sigma_{12}^{\mathrm{T}}\Sigma_{11}^{-1}\Sigma_{12} < 0$;

(3) $\Sigma_{22} < 0$ and $\Sigma_{11} - \Sigma_{12}\Sigma_{22}^{-1}\Sigma_{12}^{\mathrm{T}} < 0$.

To explain the concept of the EID, we suppose that the linear time-invariant plant with disturbance is

$$ \begin{cases} \dot{x}_o(t) = Ax_o(t) + Bu(t) + B_d d(t), \\ y_o(t) = Cx_o(t), \end{cases} \tag{6} $$

where $x_o(t)$ is the state of the plant; $u(t)$ is the control input; $y_o(t)$ is the output; $d(t)$ is a disturbance; and A, B, B_d, and C are constant matrices. If we assume that a disturbance is imposed only on the control input channel, the plant is written as

$$ \begin{cases} \dot{x}(t) = Ax(t) + B[u(t) + d_e(t)], \\ y(t) = Cx(t). \end{cases} \tag{7} $$

Definition 3 ([20]). Let the input $u(t)$ be zero. The disturbance $d_e(t)$ is called an EID of the disturbance $d(t)$ if they produce the same effect on the output, that is $y(t) \equiv y_o(t)$ for all $t \geqslant 0$.

Lemma 5 ([20]). Let $\Psi = p_i(t)\sin(\omega_i t + \psi_i)$, $i = 0,\ldots,n$, $n < \infty$, where $\omega_i \geqslant 0$ and ψ_i are constants, and $p_i(t)$ denotes any polynomials in time t $(i = 0,\ldots,n)$. If the trajectory of the output caused by the disturbance $d(t)$ is $y_o(t) \in \Psi$, then there exists an EID $d_e(t) \in \Psi$ on the control input channel that produces the same trajectory.

In this paper, we consider the following FO uncertain plant with disturbance

$$ \begin{cases} {}_0D_t^{\alpha}x(t) = [A + \Delta A(t)]x(t) + [B + \Delta B(t)][u(t) + d(t)], \\ y(t) = Cx(t), \end{cases} \tag{8} $$

where $0 < \alpha < 1$ is the fractional order, $x(t) \in \mathbb{R}^n$ is the state of the plant, $u(t) \in \mathbb{R}^p$ and $y(t) \in \mathbb{R}^q$ are the control input and output, respectively, and $d(t) \in \mathbb{R}^{n_d}$ is the disturbance. A, B and C are constant matrices of appropriate dimensions. $\Delta A(t)$ and $\Delta B(t)$ are time-variant uncertainties with the structure

$$\left[\Delta A(t) \;\; \Delta B(t) \right] = ME(t) \left[N_0 \;\; N_1 \right], \tag{9}$$

where M, N_0 and N_1 are known real matrices which characterize the structure of the uncertainty. $E(t) \in \mathbb{R}^{n \times n}$ is bounded as follows:

$$E^{\mathrm{T}}(t)E(t) \leqslant I, \quad \forall t > 0, \tag{10}$$

where the elements of $E(t)$ are Lebesgue measurable.

Remark 1. Note that the disturbance in plant (8) is in the input channel. If a disturbance is imposed on other channel except for the input one, we can also change the expression into the form in (8). In fact, as stated in [20], if the plant is controllable and observable, an EID that belongs to Ψ always exists in the control input channel of the plant. So, without loss of generality, we write FO plant with disturbance as (8).

To deal with uncertainties, we write plant (8) as

$$\begin{cases} {}_0D_t^{\alpha} x(t) = Ax(t) + Bu(t) + [\Delta A(t)x(t) + \Delta B(t)u(t) + Bd(t) + \Delta B(t)d(t)], \\ y(t) = Cx(t). \end{cases} \tag{11}$$

The uncertainties caused by the model mismatch between the identified model and the real process can be considered as an additional disturbance introduced into the system [21]. So, we treat both the uncertainties and the disturbances in the bracket in plant (11) as a whole disturbance, and compensate for the whole disturbance in the next section.

3 Main results

First, we construct the configuration of the FO control system. We use the following FO Luenberger-type state observer of the same order as the plant

$$\begin{cases} {}_0D_t^{\alpha} \hat{x}(t) = \hat{A}\hat{x}(t) + Bu_f(t) + L[y(t) - \hat{y}(t)], \\ \hat{y}(t) = C\hat{x}(t), \end{cases} \tag{12}$$

where $\hat{x}(t)$ is the observer state, and gains L and $\hat{A}$ are to be determined. So the state feedback control law is

$$u_f(t) = K\hat{x}(t), \tag{13}$$

where K is the state feedback gain to be determined.

Remark 2. The FO observer which is with the same order as the plant is used to accurately reproduce the plant states and to estimate the disturbances. Compared with conventional observers, observer (12) contains two unknown system matrices, thus providing an opportunity to adjust the dynamical properties of the FO control system.

Let the error between the plant and the observer state be

$$\Delta x(t) = x(t) - \hat{x}(t). \tag{14}$$

As discussed in [20], the disturbance estimate is given by

$$\hat{d}(t) = B^{+}LC\left[x(t) - \hat{x}(t)\right] + u_f(t) - u(t), \tag{15}$$

where $B^{+} = (B^{\mathrm{T}}B)^{-1}B^{\mathrm{T}}$ is the Moore-Penrose generalized inverse of B.

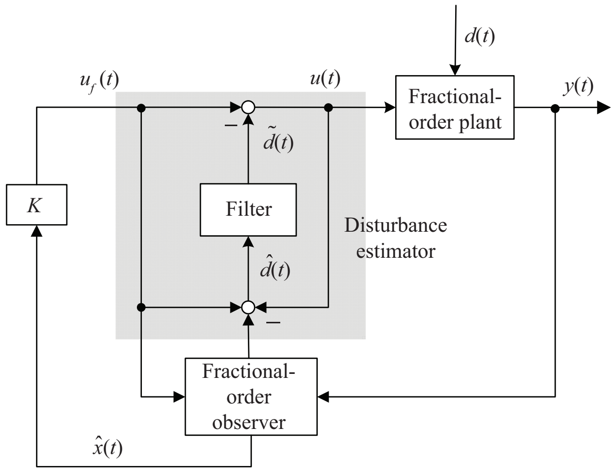

Figure 1 The configuration of the FO control system.

Since the output $y(t)$ contains measurement noise, an FO low-pass filter $F(s)$ is applied to filter the noise of the estimate. We choose an FO filter with the same order as the plant to easily formulate FO model for the control system. The filter satisfies

$$|F(j\omega)| \approx 1, \quad \forall \omega \in [0, \omega_h], \tag{16}$$

where ω_h is the highest angular frequency for the disturbance estimation. The state-space form of the filter $F(s)$ is given by

$$\begin{cases} {}_0D_t^{\alpha} x_F(t) = A_F x_F(t) + B_F \hat{d}(t), \\ \tilde{d}(t) = C_F x_F(t), \end{cases} \tag{17}$$

where $x_F(t)$ is the filter state, $\hat{d}(t)$ and $\tilde{d}(t)$ denote by the estimates before and after filtering, respectively.

Thus, the configuration of the FO control system for disturbance rejection is shown in Figure 1. Incorporating the EID estimate actively compensates for the whole disturbance and achieves better control performance for an FOS. Correspondingly, the control input is

$$u(t) = u_f(t) - \tilde{d}(t). \tag{18}$$

To analyze the stability of the control system in Figure 1, we first let the external disturbance $d(t)$ be zero.

Substituting (14) into (12) yields

$${}_0D_t^{\alpha} \hat{x}(t) = \hat{A}\hat{x}(t) + LC\Delta x(t) + Bu_f(t). \tag{19}$$

Combining (8), (12), (14) and (18) yields

$${}_0D_t^{\alpha} \Delta x(t) = [A + \Delta A(t) - \hat{A}]\hat{x}(t) + [A + \Delta A(t) - LC]\Delta x(t) - [B + \Delta B(t)]C_F x_F + \Delta B(t) u_f(t). \tag{20}$$

From (15), (17) and (18), we obtain the expression of the filter state

$${}_0D_t^{\alpha} x_F(t) = B_F B^{+} LC\Delta x(t) + (A_F + B_F C_F) x_F(t). \tag{21}$$

Define

$$\varphi(t) = \begin{bmatrix} \hat{x}^{\mathrm{T}}(t) & \Delta x^{\mathrm{T}}(t) & x_F^{\mathrm{T}}(t) \end{bmatrix}^{\mathrm{T}}. \tag{22}$$

Combining (13), (19)–(21) yields the model of the FO control system

$${}_0D_t^{\alpha} \varphi(t) = \bar{A}\varphi(t), \tag{23}$$

where

$$\bar{A} = \begin{bmatrix} \hat{A}+BK & LC & 0 \\ A+\Delta A(t)-\hat{A}+\Delta B(t)K & A+\Delta A(t)-LC & -BC_F-\Delta B(t)C_F \\ 0 & B_F B^{+} LC & A_F+B_F C_F \end{bmatrix}.$$

Assume that the singular value decomposition (SVD) of matrix C with full-row rank is

$$C = U\,[S\ \ 0]\,V^{\mathrm{T}}, \tag{24}$$

where U and V are orthogonal matrices, and S is a semi-positive definite matrix. Then partition matrix V as $V = [\,V_1\ \ V_2\,]$.

Theorem 1. FOS (23), $0 < \alpha < 1$, is asymptotically stable, if there exist symmetric positive definite matrices X_1, X_{11}, X_{22} and X_3, and appropriate matrices W_1, W_2, W_3, together with a positive scalar ε, such that the following LMI is feasible:

$$\Phi = \begin{pmatrix} \Phi_{11} & \Phi_{12} & 0 & \Phi_{14} \\ * & \Phi_{22} & \Phi_{23} & \Phi_{24} \\ * & * & \Phi_{33} & \Phi_{34} \\ * & * & * & -\varepsilon I \end{pmatrix} < 0, \tag{25}$$

where

$$\begin{aligned}
\Phi_{11} &= W_3 + W_3^{\mathrm{T}} + BW_1 + W_1{}^{\mathrm{T}}B^{\mathrm{T}}, \\
\Phi_{12} &= W_2C + X_1A^{\mathrm{T}} - W_3^{\mathrm{T}}, \\
\Phi_{14} &= X_1N_0^{\mathrm{T}} + W_1^{\mathrm{T}}N_1^{\mathrm{T}}, \\
\Phi_{22} &= AX_2 + X_2A^{\mathrm{T}} - W_2C - C^{\mathrm{T}}W_2{}^{\mathrm{T}} + \varepsilon MM^{\mathrm{T}}, \\
\Phi_{23} &= -BC_FX_3 + C^{\mathrm{T}}W_2^{\mathrm{T}}B^{+T}B_F^{\mathrm{T}}, \\
\Phi_{24} &= X_2N_0^{\mathrm{T}}, \\
\Phi_{33} &= (A_F + B_FC_F)X_3 + X_3(A_F + B_FC_F)^{\mathrm{T}}, \\
\Phi_{34} &= -X_3C_F^{\mathrm{T}}N_1^{\mathrm{T}},
\end{aligned}$$

and $X_2 = V_1X_{11}V_1^{\mathrm{T}} + V_2X_{22}V_2^{\mathrm{T}}$.

Moreover, the gains of the state feedback and that of the FO observer are given by

$$K = W_1X_1{}^{-1}, \quad L = W_2USX_{11}^{-1}S^{-1}U^{\mathrm{T}}, \quad \hat{A} = W_3X_1^{-1}. \tag{26}$$

Proof. In terms of Lemma 1, the equivalent model of (23) is

$$\begin{cases} \dfrac{\partial Z(\omega,t)}{\partial t} = -\omega Z(\omega,t) + \bar{A}\varphi(t), \\ \varphi(t) = \int_0^\infty \mu(\omega)Z(\omega,t)\mathrm{d}\omega. \end{cases} \tag{27}$$

Define a Lyapunov functional candidate as

$$V(t) = \int_0^\infty \mu(\omega)\mathrm{Z}^{\mathrm{T}}(\omega,t)P\mathrm{Z}(\omega,t)\mathrm{d}\omega, \tag{28}$$

where $P = \mathrm{diag}\{P_1, P_2, P_3\}$. P_1, P_2 and P_3 are positive definite matrices to be determined.

Taking along the solution trajectories of (27), the time derivative of $V(t)$ is

$$\begin{aligned}
\dot{V}_1(t) = &\int_0^\infty \mu(\omega)[-\omega\mathrm{Z}^{\mathrm{T}}(\omega,t) + \varphi^{\mathrm{T}}(t)\bar{A}^{\mathrm{T}}]P\mathrm{Z}(\omega,t)\mathrm{d}\omega \\
&+ \int_0^\infty \mu(\omega)\mathrm{Z}^{\mathrm{T}}(\omega,t)P[-\omega\mathrm{Z}(\omega,t) + \bar{A}\varphi(t)]\mathrm{d}\omega
\end{aligned}$$

$$= -2\int_0^{\infty} \omega\mu(\omega)\mathrm{Z}^{\mathrm{T}}(\omega,t)P\mathrm{Z}(\omega,t)\mathrm{d}\omega + \varphi^{\mathrm{T}}(t)\bar{A}^{\mathrm{T}}P\varphi(t) + \varphi^{\mathrm{T}}(t)P\bar{A}\varphi(t). \tag{29}$$

Thus, $\dot{V}_1(t) < 0$, which implies that system (27) is asymptotically stable, if

$$\bar{A}^{\mathrm{T}}P+P\bar{A}< 0. \tag{30}$$

By separating certain and uncertain parts of the system matrices in (30), we obtain

$$\begin{bmatrix} H_{11} & H_{12} & 0 \\ * & H_{22} & H_{23} \\ * & * & H_{33} \end{bmatrix} + [\Omega\bar{E}(t)\Psi + \Psi^{\mathrm{T}}\bar{E}(t)^{\mathrm{T}}\Omega^{\mathrm{T}}] < 0, \tag{31}$$

where

$$\begin{aligned}
H_{11} &= P_1\hat{A} + P_1BK + \hat{A}^{\mathrm{T}}P_1 + K^{\mathrm{T}}B^{\mathrm{T}}P_1,\\
H_{12} &= P_1LC + A^{\mathrm{T}}P_2 - \hat{A}^{\mathrm{T}}P_2,\\
H_{22} &= P_2A - P_2LC + A^{\mathrm{T}}P_2 - C^{^{\mathrm{T}}}L^{\mathrm{T}}P_2,\\
H_{23} &= -P_2BC_F + C^{\mathrm{T}}L^{\mathrm{T}}B^{+^{\mathrm{T}}}B_F^{\mathrm{T}}P_3,\\
H_{33} &= P_3(A_F + B_FC_F) + (A_F + B_FC_F)^{\mathrm{T}}P_3,\\
\Omega &= \begin{bmatrix} 0 & 0 & 0 \\ 0 & P_2M & 0 \\ 0 & 0 & 0 \end{bmatrix}, \quad \bar{E}(t) = \begin{bmatrix} E(t) & 0 & 0 \\ 0 & E(t) & 0 \\ 0 & 0 & E(t) \end{bmatrix},\\
\Psi &= \begin{bmatrix} 0 & 0 & 0 \\ N_0{+}N_1K & N_0 & -N_1C_F \\ 0 & 0 & 0 \end{bmatrix}.
\end{aligned}$$

Since $\bar{E}(t)^{\mathrm{T}}\bar{E}(t) \leqslant I$ holds for all t, from Lemma 2, Eq. (31) can be expressed as

$$\begin{bmatrix} H_{11} & H_{12} & 0 \\ * & H_{22} & H_{23} \\ * & * & H_{33} \end{bmatrix} + \varepsilon\Omega\Omega^{\mathrm{T}} + \varepsilon^{-1}\Psi^{\mathrm{T}}\Psi < 0, \tag{32}$$

where $\varepsilon > 0$.

From Lemma 4, Eq. (32) is equivalent to

$$\begin{bmatrix} H_{11} & H_{12} & 0 & N_0^{\mathrm{T}} + K^{\mathrm{T}}N_1^{\mathrm{T}} \\ * & H_{22} + \varepsilon P_2MM^{\mathrm{T}}P_2 & H_{23} & N_0^{\mathrm{T}} \\ * & * & H_{33} & -C_F^{\mathrm{T}}N_1^{\mathrm{T}} \\ * & * & * & -\varepsilon I \end{bmatrix} < 0. \tag{33}$$

To turn (33) into an LMI, first, pre- and post-multiply (33) by

$$\mathrm{diag}\{P_1{}^{-1}, P_2{}^{-1}, P_3{}^{-1}, I\} = \mathrm{diag}\{X_1, X_2, X_3, I\}. \tag{34}$$

Then, we decompose X_2 as

$$X_2 = V\mathrm{diag}\{X_{11}, X_{22}\}V^{\mathrm{T}}. \tag{35}$$

Assume that $CX_2 = \bar{X}_2C$. Combining Lemma 3 and Eq. (24) yields

$$\bar{X}_2 = USX_{11}S^{-1}U^{-1}. \tag{36}$$

Let

$$KX_1 = W_1, \quad L\bar{X}_2 = W_2, \quad \hat{A}X_1 = W_3. \tag{37}$$

Therefore, by combining (33)–(37), we obtain LMI (25) and Gains (26).

Remark 3. The use of the pending matrix $\hat{A}$ in the FO observer provides more freedom for LMI (25), which makes it easier to find a feasible solution of LMI (25).

Remark 4. In the proof of Theorem 1, the Lyapunov functional candidate is constructed using real states of the equivalent continuous frequency model. So, compared with FO Lyapunov method, it is less conservative. On the other hand, the design procedure is simple. We only need to solve an LMI (25) to obtain the controller gains, and LMI (25) is not large. Therefore, this method avoids calculation problems caused by a large partitioned matrix.

4 Simulation verification

In this section, a numerical example and a practical example are given to demonstrate the validity of the presented method for FOSs. Meanwhile, comparison simulations over the observer-based method and the IO controllers are presented to show the superiority of our method.

4.1 A numerical example

Consider the FO uncertain plant (8) with the parameters

$$A = \begin{bmatrix} -9 & 2 \\ -4 & -16 \end{bmatrix}, \quad B = \begin{bmatrix} 1.2 \\ 0.6 \end{bmatrix}, \quad C = \begin{bmatrix} 1 & 0 \end{bmatrix}, \quad \alpha = 0.9, \tag{38}$$

and the uncertainties

$$\begin{cases} M = \begin{bmatrix} 1 & 0 \\ 0 & 1 \end{bmatrix}, \ N_0 = \begin{bmatrix} 1 & 0.2 \\ 0.1 & 4 \end{bmatrix}, \ N_1 = \begin{bmatrix} 0.1 \\ 0.1 \end{bmatrix}, \\ E(t) = \mathrm{diag}\{\sin(2\pi t), \sin(2\pi t)\}. \end{cases} \tag{39}$$

Plant (38) is controllable and observable.

Let a step disturbance impose on the plant at $t = 2$ s,

$$d_1(t) = 1(t-2). \tag{40}$$

The FO filter is selected as

$$F(s) = \frac{100}{s^{\alpha} + 101} \tag{41}$$

to meet condition (16). So the parameters of the state space expression (17) are

$$A_F = -101, \quad B_F = 100, \quad C_F = 1. \tag{42}$$

Calculate the SVD of the matrix C. In terms of Theorem 1, the controller gains are derived by solving LMI (25) using MATLAB Toolbox.

$$K_1 = \begin{bmatrix} -1.7609 & -28.3317 \end{bmatrix}, \quad L_1 = \begin{bmatrix} 5.1709 \\ -10.0729 \end{bmatrix}, \quad \hat{A}_1 = \begin{bmatrix} 2.3542 & 23.6367 \\ 5.2410 & 8.9842 \end{bmatrix}. \tag{43}$$

The output response and control input for Disturbance (40) are shown in Figures 2 and 3, respectively. The presented method achieves good disturbance rejection performance for an FOS with uncertainties. The largest tracking error of the output response is less than 0.1, and converges to the starting point at approximately 11 s.

To further verify the superiority of the proposed method, we added the following disturbance with different frequencies to the plant

$$d_2(t) = 0.3(\sin 0.5\pi t + \sin 0.8\pi t) - 0.2. \tag{44}$$

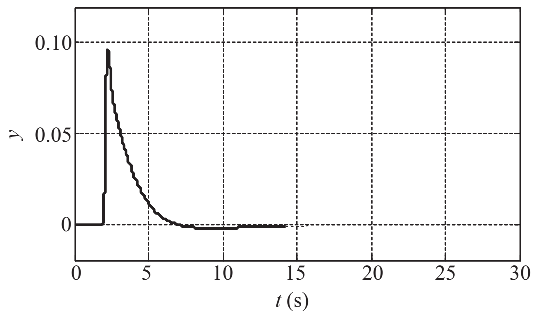

Figure 2 Output response for plant (38) with disturbance (40).

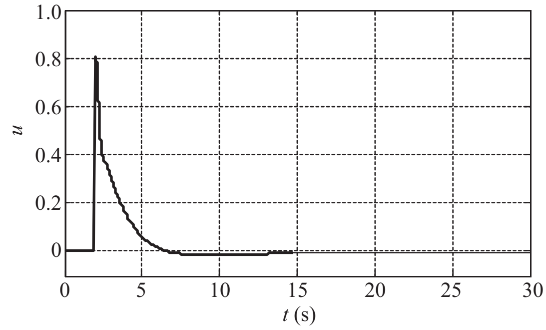

Figure 3 Control input for plant (38) with disturbance (40).

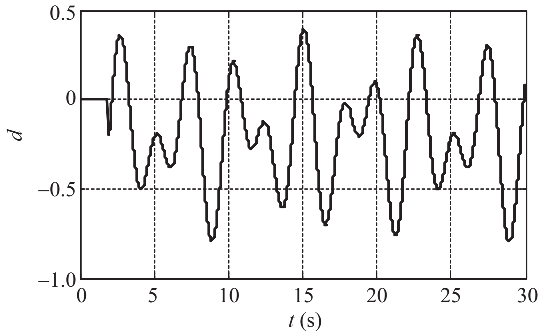

Figure 4 Disturbance (44).

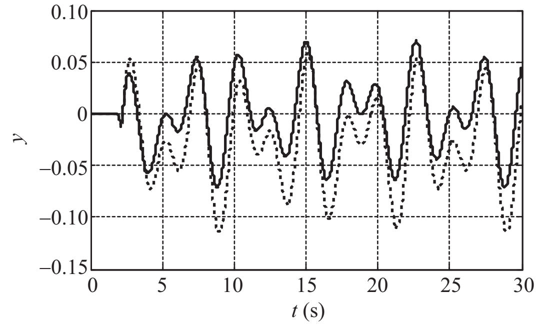

Figure 5 Outputs comparison between our method (the real line) and the observer-based method (the dotted line).

Table 1 Comparison of disturbance rejection results

Output y	Peak-to-peak value	Math. expectation	Standard deviation
Disturbance (44)	1.200	−0.184	0.298
Observer-based method	0.174	−0.026	0.043
EID-based method	0.141	−0.002	0.034

We used our method and the observer-based method [25] for comparison. The difference between these two methods lies in the disturbance estimator, which actively compensates for the whole disturbance. Figure 4 shows disturbance (44). The comparison results are shown in Figure 5. The corresponding data of the comparative results are listed in Table 1. Our method clearly achieves better control performance than the observer-based method. The average tracking error decreased by 92%.

Remark 5. External disturbances and modeling uncertainties are also treated as "total disturbance" in the ADRC method, and they are estimated using ESO. This is different from the disturbance estimator in this paper. The gains of the ESO are chosen large enough to achieve good disturbance rejection performance of the system. But measurement noise will be enhanced due to large gains, which influences the control performance. On contrast, our method achieves satisfactory control performance without requiring large gains for the FO observer.

4.2 A practical example

Heating process constantly occurs in an FO, especially when heat conduction occurs between the operating and measured physical variables. In [26], a temperature control system for a titanium billet furnace was identified as a well-controlled FO model. In this part, we consider one of the heating areas in a titanium

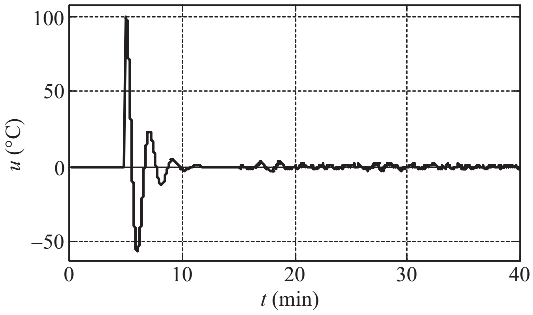

Figure 6 Control input for plant (46) affected by disturbance (48) and a white noise.

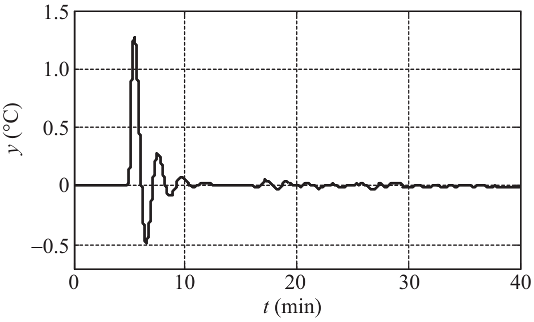

Figure 7 Output response for plant (46) affected by disturbance (48) and a white noise.

billet furnace with delay set to zero. The process was identified as

$$G(s) = \frac{1}{27.593s^{0.879} + 1}. \tag{45}$$

So the parameters for state-space model (8) are

$$A = -\frac{1}{27.593}, \quad B = \frac{1}{27.593}, \quad C = 1, \quad \alpha = 0.879. \tag{46}$$

The uncertainties were assumed to be

$$M = 1, \quad N_0 = -0.031, \quad N_1 = 0.003, \quad E(t) = \sin(0.5\pi t). \tag{47}$$

And this heating area was influenced by the following external disturbance at $t = 5$ min:

$$d_3(t) = 100(t - 5). \tag{48}$$

Then, we consider the temperature control for this heating area. The parameters of the filter are also chosen as (42). Solving LMI (25) yields the following control parameters:

$$K_2 = -9.6707, \quad L_2 = 0.0652, \quad \hat{A}_2 = -0.5208. \tag{49}$$

Since the output of the system contains measurement noise, we consider that plant (46) is affected by both disturbance (48) and a white noise (assumed power: 10^{-4}). Figure 6 shows the control input. The control temperature is between −56°C and 100°C. The output response is shown in Figure 7. It is clear that the EID-based FO control system handles large uncertainties and rejects disturbances very well. The maximal temperature fluctuation is less than 1.4°C, and the output reaches the balance temperature within 7 min. Moreover, the FO filter plays an important part in filtering high frequency noise. So the noise in the control system is also well processed, and the peak value of the output is only 0.05°C (the original peak value of the white noise is 0.4).

In order to illustrate the advantage of the proposed FO controller over the IO controller, we carry out two more simulations for comparison. First, since the control system in [21] has the same configuration as it does in this paper, we use the method in [21] to obtain the IO control parameters. The obtained parameters are $K_3 = -11.9059$, $L_3 = 0.0103$ and $\hat{A}_3 = A = -0.0362$. The dotted curve in Figure 8 shows the output response. It is obvious that the disturbance rejection performance is much better using our method (the real curve). Second, we use the same parameters as (49) and simulate applying IO observer and filter in the control system. Compared with our FO controller, the IO controller (conventional EID) shows larger overshoot and longer settling time in rejecting the disturbance. Therefore, the FO observer with the same order as the plant reproduces states of the plant and estimates disturbances of the system more accurately.

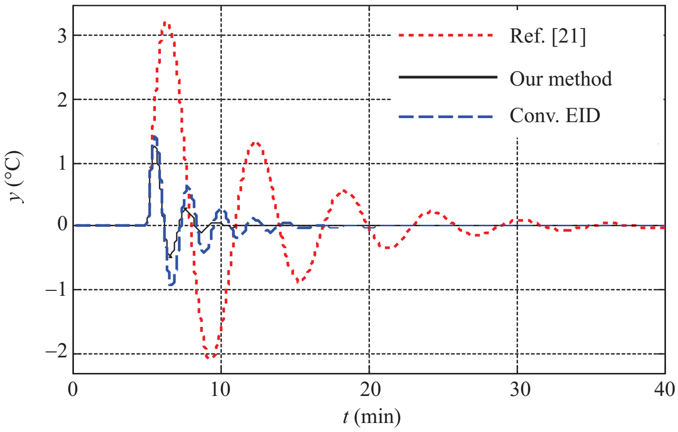

Figure 8 (Color online) Output responses for plant (46) with disturbance (48) for the method in [21], our method, and the conventional EID method.

5 Conclusion

A disturbance rejection method based on the EID approach is presented for the FOS. A robust stability condition and the parameters of the controller are derived using an indirect Lyapunov method. External disturbances and modeling uncertainties are compensated well under the construction of the EID-based FO control system. The advantages of our method are as follows:

(1) Our method not only rejects unknown disturbances effectively, but also processes noise well for an uncertain FO system.

(2) The proposed technique effectively rejects any disturbance without requiring prior information about the latter.

(3) The design procedure is simple and avoids using large observer gains to achieve satisfactory disturbance rejection performance.

Comparison simulations demonstrate that the presented method is feasible and efficient.

Acknowledgements This work was supported by National Natural Science Foundation of China (Grant Nos. 11626200, 61403149), Fujian Provincial Natural Science Foundation (Grant Nos. 2016J05165, 2015J01261), Promotion Program of Huaqiao University (Grant No. ZQN-PY408), Hubei Provincial Natural Science Foundation (Grant No. 2015CFA010), and 111 Project (Grant No. B17040).

References

1 Chen Y Q. Ubiquitous fractional order controls. In: Proceedings of the 2nd IFAC Workshop on Fractional Differentiation and Its Applications, Porto, 2006. 19–21

2 Wang J F. Control Performance Analysis for Fractional Order Systems. Beijing: Publishing House Of Electronics Industry, 2010

3 Podlubny I. Fractional-order systems and pid controllers. IEEE Trans Automat Contr, 1999, 44: 208–214

4 Oustaloup A, Bansard M. First generation CRONE control. In: Proceedings of Conference on System, Man and Cybernetic, Systems Engineering in the Service of Humans, 1993. 130–135

5 Matignon D. Stability results for fractional differential equations with applications to control processing. Comput Eng Syst Appl, 1996, 2: 963–968

6 Sabatier J, Moze M, Farges C. LMI stability conditions for fractional order systems. Comput Math Appl, 2010, 59: 1594–1609

7 Lu J-G, Chen G R. Robust stability and stabilization of fractional-order interval systems: an LMI approach. IEEE Trans Automat Contr, 2009, 54: 1294–1299

8 Li Y, Chen Y Q, Podlubny I. Stability of fractional-order nonlinear dynamic systems: Lyapunov direct method and generalized Mittag-Leffler stability. Comput Math Appl, 2010, 59: 1810–1821

9 Trigeassou J C, Maamri N, Sabatier J, et al. A Lyapunov approach to the stability of fractional differential equations. Signal Process, 2011, 91: 437–445

10 Lan Y H, Gu H B, Chen C X, et al. An indirect Lyapunov approach to the observer-based robust control for fractional-order complex dynamic networks. Neurocomputing, 2014, 136: 235–242

11 Mujumdar A, Tamhane B, Kurode S. Observer-based sliding mode control for a class of noncommensurate fractional-order systems. IEEE/ASME Trans Mechatron, 2015, 20: 2504–2512
12 Hosseinnia S H, Ghaderi R, Ranjbar N A, et al. Sliding mode synchronization of an uncertain fractional order chaotic system. Comput Math Appl, 2010, 59: 1637–1643
13 Gao Z. Active disturbance rejection control for nonlinear fractional-order systems. Int J Robust Nonlinear Control, 2016, 26: 876–892
14 Gao Z, Liao X. Active disturbance rejection control for synchronization of different fractional-order chaotic systems. In: Proceedings of Intelligent Control and Automation, Shenyang, 2015. 2699–2704
15 Wei Y, Chen Y, Liang S, et al. A novel algorithm on adaptive backstepping control of fractional order systems. Neurocomputing, 2015, 165: 395–402
16 Li M, Li D, Wang J, et al. Active disturbance rejection control for fractional-order system. ISA Trans, 2013, 52: 365–374
17 Li D, Ding P, Gao Z. Fractional active disturbance rejection control. ISA Trans, 2016, 62: 109–119
18 Fedele G, Ferrise A. Periodic disturbance rejection for fractional-order dynamical systems. Fractional Calculus Appl Anal, 2015, 18: 603–620
19 Pashaei S, Badamchizadeh M. A new fractional-order sliding mode controller via a nonlinear disturbance observer for a class of dynamical systems with mismatched disturbances. ISA Trans, 2016, 63: 39–48
20 She J H, Fang M, Ohyama Y, et al. Improving disturbance-rejection performance based on an equivalent-input-disturbance approach. IEEE Trans Ind Electron, 2008, 55: 380–389
21 She J, Wu M, Liu R J, et al. Robust disturbance rejection based on equivalent-input-disturbance approach. IET Control Theor Appl, 2013, 7: 1261–1268
22 Li X, de Souza C E. Delay-dependent robust stability and stabilization of uncertain linear delay systems: a linear matrix inequality approach. IEEE Trans Automat Contr, 1997, 42: 1144–1148
23 Ho D W C, Lu G. Robust stabilization for a class of discrete-time non-linear systems via output feedback: the unified LMI approach. Int J Control, 2003, 76: 105–115
24 Khargonekar P P, Petersen I R, Zhou K. Robust stabilization of uncertain linear systems: quadratic stabilizability and H/sup infinity / control theory. IEEE Trans Automat Contr, 1990, 35: 356–361
25 Lan Y H, Huang H X, Zhou Y. Observer-based robust control of a $(1 \leqslant a < 2)$ fractional-order uncertain systems: a linear matrix inequality approach. IET Control Theor Appl, 2012, 6: 229–234
26 Nie Z, Wang Q, Liu R. Identification and PID control for a class of delay fractional-order systems. IEEE/CAA J Autom Sin, 2016, 3: 463–476